RESEARCH PAPER



Magnesium dendrite growth during electrodeposition in conditioned Mg(TFSI)₂/AlCl₃/MgCl₂/DME electrolyte

Lin Wang · Peter Chun Pang Li · Roxana Family · Eric Detsi

Received: 24 July 2023 / Accepted: 26 November 2023 / Published online: 19 December 2023 © The Author(s), under exclusive licence to Springer Nature B.V. 2023

Abstract Mg-ion batteries (MIBs) have emerged as a promising alternative to Li-ion batteries (LIBs) since Mg metal is more abundant, cheaper, and safer than Li metal. However, the growth of Mg dendrites on metal Mg anodes is still very controversial, while several studies claim that Mg dendrites do not form on Mg metal anodes; other studies claim the opposite. Recently, a new class of MIB electrolytes which we refer to here as MACT has received extensive attention due to its higher ionic conductivity and wider potential window. MACT is made of magnesium bis(trifluoromethanesulfonyl)imide (Mg(TFSI)₂), aluminum chloride (AlCl₃), and magnesium chloride (MgCl₂) in 1,2-dimethoxyethane (DME). Previous studies have claimed that Mg dendrites do not grow in conditioned MACT electrolytes. This article explores the formation of magnesium (Mg) dendrites in a conditioned MACT electrolyte during electrodeposition. A symmetric cell configuration, MglMACTlMg, was utilized to investigate the dendrite formation at different current densities. The morphology, chemical composition, and crystal structure of the deposition products were characterized using scanning electron microscopy (SEM), energy dispersive X-ray spectroscopy (EDS), and X-ray diffraction (XRD). Our findings demonstrate the growth of Mg dendrites within the MACT electrolyte. We observed that the morphology of these dendrites undergoes evolution with varying the electrodeposition current density, transitioning between mossy clusters, granular structures, and porous mesh formations in a size range from approximately 10 to 125 µm. These results significantly enhance our understanding of Mg dendrite formation in MIBs.

Keywords Mg-ion battery · Mg dendrites · Plating/ stripping · Morphology · Nanoscale interfaces · Energy storage

This manuscript is part of the Special Collection on "Nanomanufacturing"

Supplementary Information The online version contains supplementary material available at https://doi.org/10.1007/s11051-023-05905-0.

L. Wang · P. C. P. Li · R. Family · E. Detsi (☒) Department of Materials Science & Engineering, University of Pennsylvania, Philadelphia, PA 19104, USA e-mail: detsi@seas.upenn.edu

P. C. P. Li

Department of Physics and Astronomy, University of Pennsylvania, Philadelphia, PA 19104, USA

Introduction

Mg-ion batteries (MIBs) have attracted considerable attention as a promising alternative to Li-ion batteries (LIBs) because Mg metal is more abundant, cheaper, and safer than Li metal [1–7]. The use of Mg metal as a practical anode in MIBs is possible only if Mg dendrites do not grow during (dis)charging,



since these dendrites can penetrate through the separator and come into direct contact with the cathode, potentially causing short-circuits and safety hazards [8–10]. However, whether Mg dendrites will form remains highly controversial: (i) While several early studies including in situ scanning tunneling microscopy (in situ STM) studies [11], in situ atomic force microscopy (in situ AFM) analysis combined with optical imaging [12], and theoretical simulation [13, 14], suggested that Mg dendrites do not grow; new studies suggested the opposite. For example, Banerjee's group demonstrated the growth of Mg dendrites during electrodeposition in 0.5 M methylmagnesium chloride (MeMgCl) electrolyte in tetrahydrofuran (THF) electrolyte [15], and in 0.25 M, 0.5 M, 1.0 M, and 1.5 M MeMgCl in THF [16]; Zhang's group showed that Mg dendrites form in 0.3 M all-phenylcomplex (APC) electrolyte [17]; Lim's group also visualized the growth of Mg dendrites in APC electrolytes [18]. (ii) Recently, MIB electrolytes based on magnesium bis(trifluoromethanesulfonyl)imide salt— Mg(TFSI)₂—have received extensive attention due to their higher ionic conductivity and wider potential window [8, 19–24]. While Choi's group first claimed that Mg dendrites do not form in Mg(TFSI)₂-based electrolytes such as 0.3 M Mg(TFSI)₂ in glyme/ diglyme [19]; Giffin's group observed the growth of Mg dendrites in 0.3 M Mg(TFSI)₂ in glyme [8]. Meanwhile, many other studies claimed that Mg dendrites do not form in hybrid Mg(TFSI)₂/aluminum chloride (AlCl₃)/magnesium chloride (MgCl₂) in 1, 2-dimethoxyethane (DME) electrolytes [21–24]. The hybrid Mg(TFSI)₂/AlCl₃/MgCl₂/DME is abbreviated in this article as MACT.

The aim of this study is to verify whether Mg dendrites will form in a conditioned MACT electrolyte. With this aim in mind, we electrodeposited Mg in galvanostatic mode at various current densities using a symmetric MglMACTlMg cell, visualized and recorded the deposition products. In our study, we employed scanning electron microscopy (SEM) for visualizing the morphology, energy dispersive X-ray spectroscopy (EDS) for determining the elemental composition, and X-ray diffraction (XRD) for analyzing the crystalline phases of the deposited products across varying current densities. Our findings present compelling evidence of dendrite formation on Mg metal anodes within conditioned MACT electrolytes. Moreover, our results strongly indicate that

the morphology of Mg dendrites is influenced by the applied electrodeposition current density.

Experimental

Materials and chemicals

A 0.1-mm thick magnesium (Mg) foil with a purity of 99.9% was purchased from MTI Corporation, serving as the working, counter, and reference electrodes. Magnesium (II) bis(trifluoromethanesulfonyl) imide—Mg(TFSI)₂—with 99.5% purity was purchased from Solvionic and dried overnight at 150 °C to remove residual moisture. Aluminum trichloride (AlCl₃, 99.985%) and magnesium chloride (MgCl₂, 99.99%) were purchased from Alfa-Aesar and used without further purification. Anhydrous 1, 2-dimethoxyethane (DME, 99.5%) was purchased from Sigma-Aldrich and dried for 72 hours using activated molecular sieves with a pore size of 4 Å for 72 hours. All materials and chemicals were stored in an argon-filled glovebox (< 0.1 ppm H₂O and O₂).

Electrolyte and cell preparation

MACT electrolyte with a concentration of 0.25 M is composed of 0.25 M Mg(TFSI)₂, 0.25 M AlCl₃, and 0.5 M MgCl₂ with a molar ratio of 1:1:2 in DME. To prepare 10 mL of 0.25 M MACT electrolyte, 0.005 mol (476 mg) of MgCl₂ was added to 10 mL of dried DME solvent in an argon-filled glovebox. Then 0.0025 mol (333 mg) of AlCl₃ was added in a round bottom flask with a rubber stopper on. About 0.5 M MgCl₂ in DME was added to the round bottom flask drop by drop. Then, 0.0025 mol (1.46 g) of Mg(TFSI)₂ was added while stirring. The electrolyte was stirred overnight to mix fully. The MACT electrolyte was then conditioned before use by running cyclic voltammetry (CV) experiments at the scan rate of 1 mV s⁻¹, and the voltage window was from -1V to 1 V using a MglMACTlMg cell configuration with a polished Mg foil as the working electrode, and another polished Mg foil as the counter and reference electrodes until stable CV curves were achieved [18, 21]. The MACT electrolyte performance is improved after conditioning through the removal of possible impurities [21]. In Fig. S1, we present the selected CV curves during the conditioning process of MACT



J Nanopart Res (2024) 26:1 Page 3 of 7 1

electrolyte. These CV scans, conducted at a scan rate of 1 mV s $^{-1}$ within the potential range of -0.8 to 2.0 V, clearly demonstrate the improved reversibility of the Mg deposition process over consecutive cycles, from light blue to dark blue curves. This enhancement is evident through reduced overpotentials and higher cycling efficiencies. The MglMACTIMg symmetric cell (with 0.25 M-conditioned MACT electrolyte) was used for subsequent experiments. A schematic of this cell is shown in Fig. 1 a, with the corresponding accurate picture shown in Fig. 1 b. The distance between two Mg foils is approximately 1 cm. All experiments are conducted in an argon-filled glovebox with residual O_2 and H_2O below 0.1 ppm.

Electrochemical characterization

Electrochemical tests were performed using a Bio-Logic VMP-300 multichannel potentiostat. The MglMACTlMg symmetric cell was cycled between -3 and 1 V in galvanostatic mode using different areal current densities while keeping the areal capacity constant by varying the cycling time.

Material characterization

Scanning electron microscopy (SEM) images were captured using a JEOL 7500F high-resolution scanning electron microscope. For morphology and compositional analysis, energy dispersive X-ray spectroscopy (EDS) was performed using an Octane Elect Super detector. X-ray diffraction (XRD) patterns were obtained on a Rigaku Miniflex powder diffractometer, equipped with a Cu X-ray source operating at 40 kV

size of 0.01° and a scanning speed of 5°/min.

Results and discussion

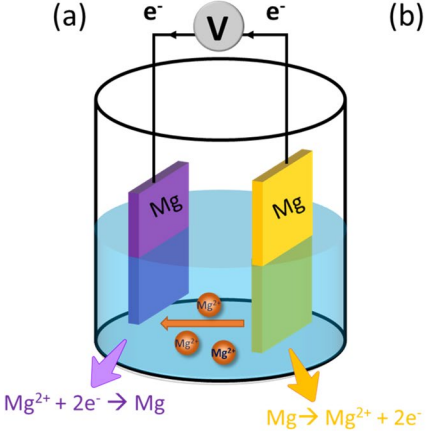
To investigate the formation of Mg dendrite

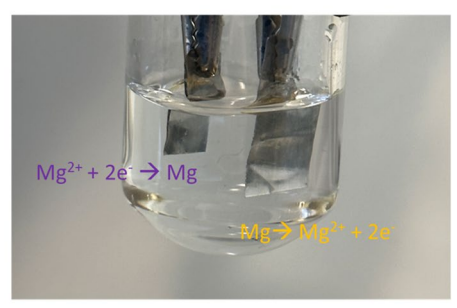
To investigate the formation of Mg dendrites in the MACT electrolyte, we conducted electrodeposition experiments using a symmetric MglMACTlMg cell. The MACT electrolyte was properly conditioned for the study. The electrodeposition of Mg was carried out at various current densities: 5, 6, 7, 8, 9, and 10 mA cm⁻². This approach allowed us to determine whether Mg dendrites were formed in the MACT electrolyte under different current density conditions.

and 15 mA. The measurements were taken with a step

The areal capacity achieved at each of these current densities is maintained constant at 10 m Ah cm⁻² by controlling the electrodeposition time. The corresponding voltage vs. capacity plots for all current densities are shown in Fig. 2 a. The relatively high negative voltage is associated with the high overpotential needed to reduce Mg ions (Mg²⁺) to metal Mg onto the working electrode through the following half reaction: $Mg^{2+} + 2e^{-} \rightarrow Mg$, with the reverse half reaction (i.e., Mg \rightarrow Mg²⁺ +2e⁻) taking place on the counter electrode. It is a striking phenomenon that the overpotential at 5 mA cm⁻² (pink curve in Fig. 2 a) is higher than others. A possible explanation is that the system initially requires high activation energy to grow Mg dendrite onto the Mg foil electrode. Once a "layer" of Mg dendrite is deposited on the Mg foil electrode, subsequent Mg dendrites are deposited on top of Mg dendrites and this may require lower activation energy. In other words, it may be kinetically

Fig. 1 (a) Schematic of the electrochemical symmetric cell setup. At the Mg foil working electrode, Mg ions accept electrons and are reduced to metal Mg (left side, purple). At the Mg foil counter and reference electrode, metal Mg lose electrons to become Mg ions (right side, yellow). (b) Image of the actual cell. The cell operates in an argon environment







1 Page 4 of 7 J Nanopart Res (2024) 26:1

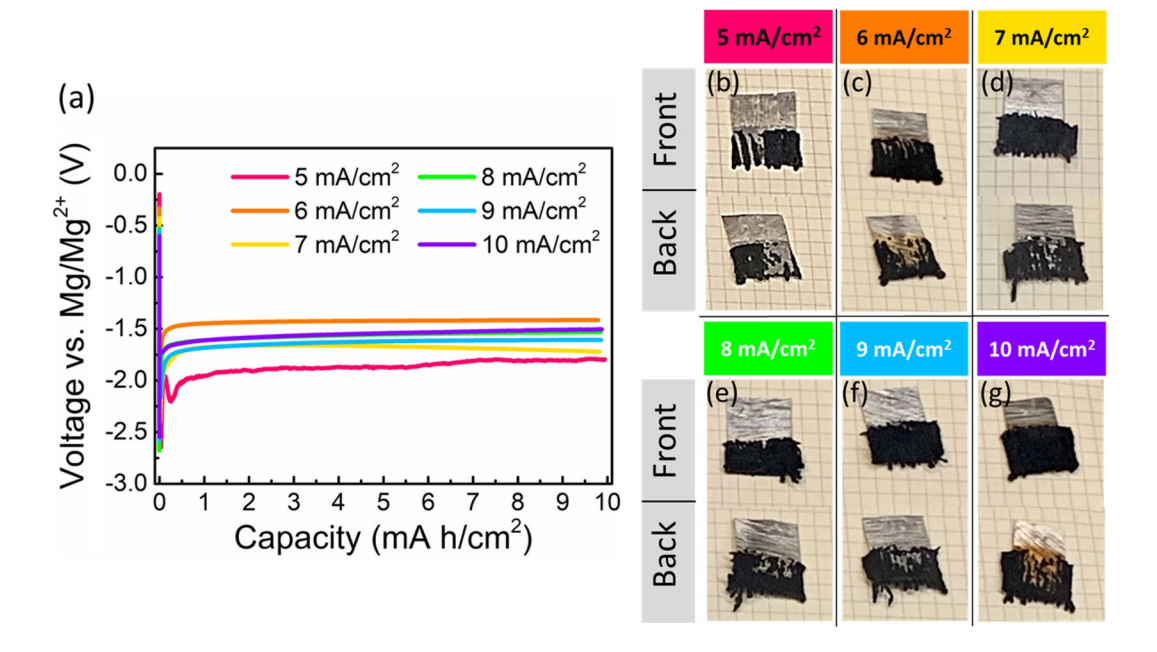


Fig. 2 (a) Voltage vs. areal capacity curves for all current densities. (b) Images of the front and back sides of the Mg foil working electrodes at different current densities

easier to grow Mg dendrites on top of Mg dendrite than growing Mg dendrites on top of Mg foil. At low current densities, Mg dendrites are grown on Mg foil. At high current densities, Mg dendrites are initially grown on the Mg foil electrode and further on Mg dendrites. The formation of Mg deposits onto the working electrode during electrodeposition was recorded for all current densities (see supporting videos S1, S2, S3, S4, S5, S6). Fig. 2 b displays representative images of the front and back sides of the Mg foil working electrodes obtained after electrodeposition at various current densities. A black deposit can be observed on each working electrode. The morphology of these deposits was investigated by SEM (Fig. 3). At 5 mA cm⁻², mossy-like deposits were observed at low magnification (Fig. 3a). The diameter of each mossy cluster was ≈125 µm. This mossylike morphology aligns well with the morphology of the Mg dendrites found by Ding et al., which similarly observed the presence of dendrites on Mg metal with Mg(TFSI)₂ in glyme electrolyte [8]. Upon closer inspection at a higher magnification (Fig. 3b), we found that the mossy-like dendrites exhibit lamellar structures with nano-sized thickness. At 6 mA cm⁻², the dendrites are still mossy-like, but with a smaller cluster diameter of $\approx 100 \mu m$, as shown in Fig. 3 c. The zoomed-in image in Fig. 3 d showed a thicker nano-sized lamellae structure. At a current density of 7 mA cm⁻², the dendrites displayed an interconnected granular morphology with grain sizes of approximately 10 µm, as depicted in Fig. 3 e and f. At an applied current density of 8 mA cm⁻², the mossy-like dendrites reemerged, characterized by a diminished cluster diameter of approximately 75 µm (Fig. 3g). Additionally, the presence of lamellar structures with a nano-sized thickness was observed (Fig. 3h). At 9 mA cm⁻², the dendrites exhibit the porous mesh structure in Fig. 3 i and j. Finally, at 10 mA cm⁻², the dendrites appear as interconnected islands with significant surface undulations. The SEM results suggest that the morphology of Mg dendrites seems to be impacted by the electrodeposition current density.

Next, the chemical composition and the crystal structure of the Mg deposition products were investigated at all current densities using EDS and XRD. Typical EDS and XRD data for Mg deposits formed at 10 mA cm⁻² are shown in Fig. 4. Note that because EDS and XRD data were similar in all current densities, here, we only show the XRD and EDS obtained at 10 mA cm⁻². In Fig. 4 a, the EDS spectrum of the Mg deposits reveals the presence of C, O, F, S, Al, Cl, and Mg signals. The Al and Cl signals were attributed



J Nanopart Res (2024) 26:1 Page 5 of 7 1

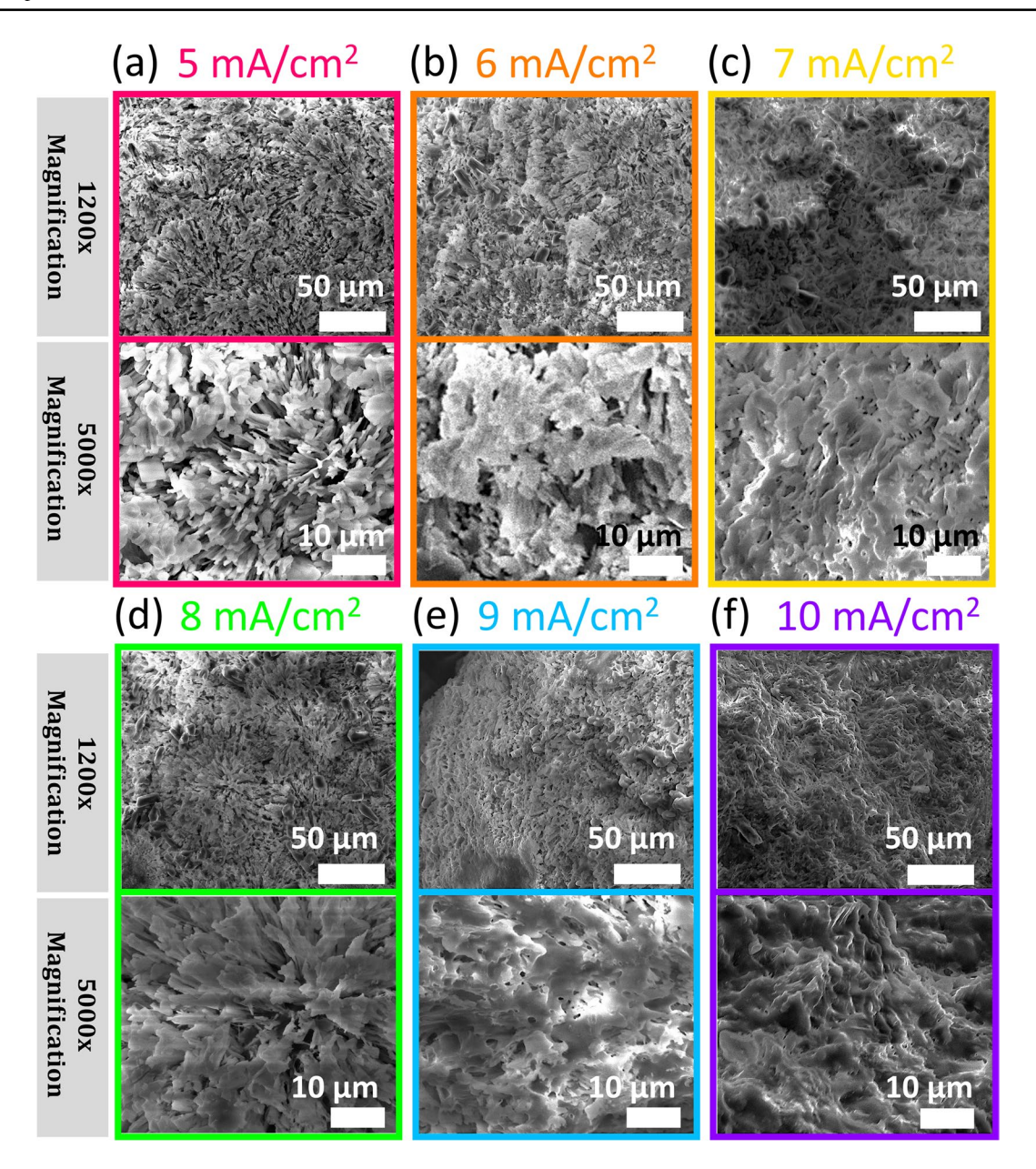


Fig. 3 SEM images of Mg dendrites formed on Mg working electrodes at **a** and **b** 5 mA cm⁻², (**c**, **d**) 6 mA cm⁻², (**e**, **f**) 7 mA cm⁻², (**g**, **h**) 8 mA cm⁻², (**i**, **j**) 9 mA cm⁻², and (**k**, **l**) 10 mA cm⁻², respectively

to AlCl₃ salt from the MACT electrolyte. The C, O, F, and S signals were ascribed to Mg (TFSI)₂ salt from the MACT. In Fig. 4 b, the XRD analysis shows the presence of Mg (PDF#35-0821), MgCl₂ (PDF#03-0854), AlCl₃ (PDF#01-1133), MgO (PDF#87-0651), MgF (PDF#70-2269), MgS (PDF#75-0897), and MgCO₃ (PDF#86-0175). The identification of MgF

and MgS within the deposited products serves as compelling evidence for the presence of a solid interfacial layer. This finding is supported by previous studies [20, 22]. However, it should be noted that the XRD data of all deposited products could not be fully fitted, likely due to the relatively lower crystallinity of certain deposition products.



1 Page 6 of 7 J Nanopart Res (2024) 26:1

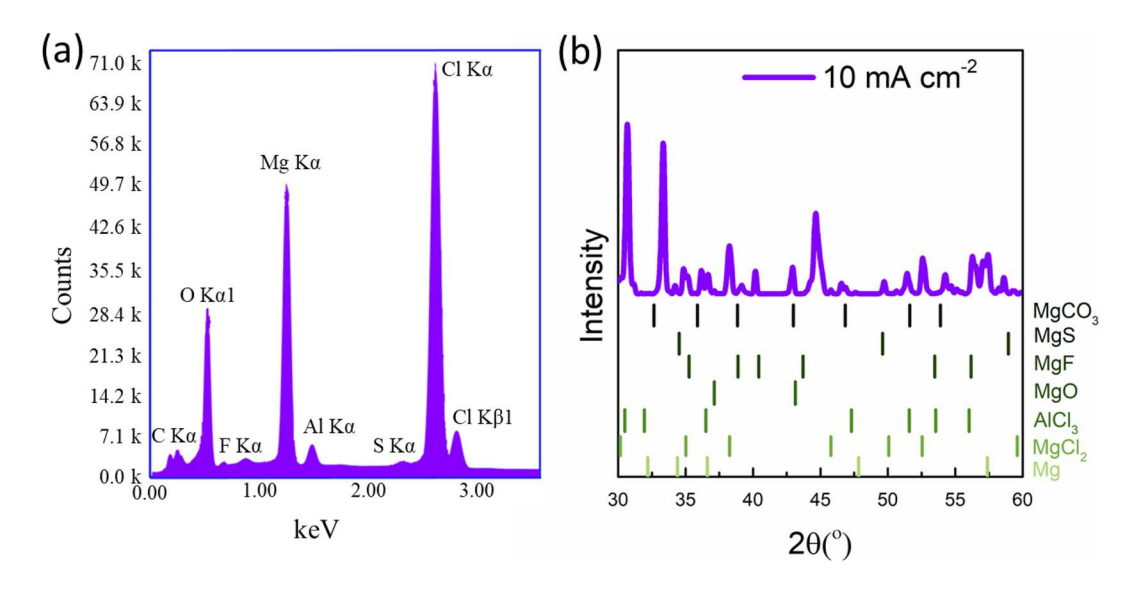


Fig. 4 Typical a EDS spectra and b XRD pattern of the deposition products formed at 10 mA cm⁻²

Conclusion

This study successfully demonstrates the formation and growth of Mg dendrites in a conditioned MACT electrolyte through electrodeposition at varying current densities. The morphology, chemical composition, and crystal structure of the resulting Mg dendrite deposits were thoroughly investigated using SEM, EDS, and XRD techniques. Our findings indicate that the morphologies of the dendrites are directly influenced by the employed current density during electrodeposition. By carefully analyzing the results, we observed distinct variations in dendrite structures corresponding to different current densities. This discovery elucidates the intricate relationship between electrodeposition parameters and resulting dendrite formations. The utilization of SEM, EDS, and XRD allowed for comprehensive characterization of the Mg dendrite deposits, providing valuable insights into their properties. These findings have significant implications for the development and optimization of electrolyte and electrodeposition processes in Mg-based electrochemical systems. In conclusion, this research expands our understanding of Mg dendrite formation and growth, emphasizing the crucial role of controlling current density in achieving desired dendrite morphologies. Further investigations should explore additional factors that may impact dendrite growth, aiming to develop strategies to mitigate or regulate dendrite formation in Mg-based systems.

Acknowledgements The authors are thankful to Yihui Zhang for collecting scanning electron microscope images.

Funding This work received financial support from the National Science Foundation (NSF), Division of Materials Research (DMR), Future Manufacturing Research Grant #2134715. This work was carried out in part at the Singh Center for Nanotechnology, which is supported by the NSF National Nanotechnology Coordinated Infrastructure Program under grant NNCI-2025608. Additional support to the Nanoscale Characterization Facility at the Singh Center has been provided by the Laboratory for Research on the Structure of Matter (MRSEC) supported by the National Science Foundation (DMR-1720530).

Compliance with ethical standards

Conflict of interest The authors declare no competing interests.

References

- Yoo HD, Shterenberg I, Gofer Y et al (2013) Mg rechargeable batteries: an on-going challenge. Energy Environ Sci 6:2265–2279. https://doi.org/10.1039/c3ee40871j
- Singh N, Arthur TS, Tutusaus O et al (2018) Achieving high cycling rates via in situ generation of active nanocomposite metal anodes. ACS Appl Energy Mater 1:4651–4661. https://doi.org/10.1021/acsaem.8b00794



J Nanopart Res (2024) 26:1 Page 7 of 7 1

Crowther O, West AC (2008) Effect of electrolyte composition on lithium dendrite growth. J Electrochem Soc 155:806–811. https://doi.org/10.1149/1.2969424

- Muldoon J, Bucur CB, Gregory T (2014) Quest for nonaqueous multivalent secondary batteries: magnesium and beyond. Chem Rev 114:11683–11720. https://doi.org/10. 1021/cr500049y
- Wang L, Welborn SS, Kumar H et al (2019) High-Rate and long cycle-life alloy-type magnesium-ion battery anode enabled through (de)magnesiation-induced nearroom-temperature solid–liquid phase transformation. Adv Energy Mater 9:1–7. https://doi.org/10.1002/aenm.20190 2086
- Niu J, Gao H, Ma W et al (2018) Dual phase enhanced superior electrochemical performance of nanoporous bismuth-tin alloy anodes for magnesium-ion batteries. Energy Storage Mater 14:351–360. https://doi.org/10. 1016/j.ensm.2018.05.023
- Wang L, Weker JN, Family R et al (2023) Morphology evolution in self-healing liquid-gallium-based Mg-ion battery anode. ACS Energy Lett:4932–4940. https://doi.org/ 10.1021/ACSENERGYLETT.3C01761
- Ding MS, Diemant T, Behm RJ et al (2018) Dendrite growth in Mg metal cells containing Mg(TFSI) 2/glyme electrolytes. J Electrochem Soc 165:A1983–A1990. https://doi.org/10.1149/2.1471809jes
- Niu J, Song M, Zhang Y, Zhang Z (2021) Dealloying induced nanoporosity evolution of less noble metals in Mg ion batteries. J Magnes Alloy 9:2122–2132. https:// doi.org/10.1016/j.jma.2021.04.003
- Niu J, Zhang Z, Aurbach D (2020) Alloy anode materials for rechargeable Mg ion batteries. Adv Energy Mater 10:2000697. https://doi.org/10.1002/AENM.202000697
- Aurbach D, Cohen Y, Moshkovich M (2001) The study of reversible magnesium deposition by in situ scanning tunneling microscopy. Electrochem Solid-State Lett 4:A113. https://doi.org/10.1149/1.1379828/XML
- Hu XC, Shi Y, Lang SY et al (2018) Direct insights into the electrochemical processes at anode/electrolyte interfaces in magnesium-sulfur batteries. Nano Energy 49:453– 459. https://doi.org/10.1016/J.NANOEN.2018.04.066
- Hagopian A, Kopač D, Filhol JS, Kopač Lautar A (2020) Morphology evolution and dendrite growth in Li- and Mg-metal batteries: a potential dependent thermodynamic and kinetic multiscale ab initio study. Electrochim Acta 353:136493. https://doi.org/10.1016/J.ELECTACTA.2020. 136493
- Jäckle M, Groß A (2014) Microscopic properties of lithium, sodium, and magnesium battery anode materials related to possible dendrite growth. J Chem Phys 141:174710. https://doi.org/10.1063/1.4901055
- Davidson R, Verma A, Santos D et al (2019) Formation of magnesium dendrites during electrodeposition. ACS

- Energy Lett 4:375–376. https://doi.org/10.1021/acsen ergylett.8b02470
- Davidson R, Verma A, Santos D et al (2020) Mapping mechanisms and growth regimes of magnesium electrodeposition at high current densities. Mater Horizons 7:843–854. https://doi.org/10.1039/c9mh01367a
- Zhao Y, Zhang X, Xiao J et al (2022) Effect of Mg cation diffusion coefficient on Mg dendrite formation. ACS Appl Mater Interfaces 14:6499–6506. https://doi.org/10.1021/ acsami.1c18543
- Kwak JH, Jeoun Y, Oh SH et al (2022) Operando visualization of morphological evolution in Mg metal anode: insight into dendrite suppression for stable Mg metal batteries. ACS Energy Lett 7:162–170. https://doi.org/10.1021/acsenergylett.1c02486
- Ha SY, Lee YW, Woo SW et al (2014) Magnesium(II) bis(trifluoromethane sulfonyl) imide-based electrolytes with wide electrochemical windows for rechargeable magnesium batteries. ACS Appl Mater Interfaces 6:4063– 4073. https://doi.org/10.1021/am405619v
- Eaves-Rathert J, Moyer K, Zohair M, Pint CL (2020) Kinetic- versus diffusion-driven three-dimensional growth in magnesium metal battery anodes. Joule 4:1324–1336. https://doi.org/10.1016/j.joule.2020.05.007
- 21. Shterenberg I, Salama M, Yoo HD et al (2015) Evaluation of (CF 3 SO 2) 2 N (TFSI) based electrolyte solutions for Mg batteries. J Electrochem Soc 162:A7118–A7128. https://doi.org/10.1149/2.0161513jes
- Yang L, Yang C, Chen Y et al (2021) Hybrid MgCl2/ AlCl3/Mg(TFSI)2 electrolytes in DME enabling high-rate rechargeable Mg batteries. ACS Appl Mater Interfaces 13:30712–30721. https://doi.org/10.1021/acsami.1c07567
- He Y, Li Q, Yang L et al (2019) Electrochemical-conditioning-free and water-resistant hybrid AlCl 3 /MgCl 2 / Mg(TFSI) 2 electrolytes for rechargeable magnesium batteries. Angew Chem 131:7697–7701. https://doi.org/10.1002/ange.201812824
- Gao T, Hou S, Wang F et al (2017) Reversible S0/MgSx redox chemistry in a MgTFSI2/MgCl2/DME electrolyte for rechargeable Mg/S batteries. Angew Chem Int Ed 56:13526–13530

Publisher's Note Springer Nature remains neutral with regard to jurisdictional claims in published maps and institutional affiliations.

Springer Nature or its licensor (e.g. a society or other partner) holds exclusive rights to this article under a publishing agreement with the author(s) or other rightsholder(s); author self-archiving of the accepted manuscript version of this article is solely governed by the terms of such publishing agreement and applicable law.

